International Journal of Nanomedicine

Dovepress
Taylor & Francis Group

Open Access Full Text Article

ORIGINAL RESEARCH

Microwave-Assisted Synthesized ZnO@APTES Quantum Dots Exhibits Potent Antibacterial Efficacy Against Methicillin-Resistant *Staphylococcus aureus* Without Inducing Resistance

Fangyuan Du[1,*], Jingqi Niu[1,*], Yu Hong[1], Xue Fang[2], Zhihui Geng[1], Jing Liu[1], Fangqi Xu[1], Tingshu Liu[1], Qifan Chen[1], Jingbo Zhai[3], Beiliang Miao[4], Shiwei Liu[4], Yi Zhang[1], Zeliang Chen[1]

[1]Key Laboratory of Livestock Infectious Diseases, Ministry of Education, and Key Laboratory of Ruminant Infectious Disease Prevention and Control (East), Ministry of Agriculture and Rural Affairs, College of Animal Science and Veterinary Medicine, Shenyang Agricultural University, Shenyang, 110866, People's Republic of China; [2]College of Animal Husbandry & Veterinary Medicine, Jinzhou Medical University, Jinzhou, 121001, People's Republic of China; [3]Key Laboratory of Zoonose Prevention and Control at Universities of Inner Mongolia Autonomous Region, Medical College, Inner Mongolia Minzu University, Tongliao, 028000, People's Republic of China; [4]Department of Nephrology and Endocrinology, Wangjing Hospital, Chinese Academy of Chinese Medical Science, Beijing, 100102, People's Republic of China

*These authors contributed equally to this work

Correspondence: Yi Zhang; Zeliang Chen, Key Laboratory of Livestock Infectious Diseases, Ministry of Education, and Key Laboratory of Ruminant Infectious Disease Prevention and Control (East), Ministry of Agriculture and Rural Affairs, College of Animal Science and Veterinary Medicine, Shenyang Agricultural University, 120 Dongling Road, Shenyang, 110866, Liaoning, People's Republic of China, Email 2005500042@syau.edu.cn; chenzliang5@mail.sysu.edu.cn

Background: Antibiotic resistance of many bacteria, including Methicillin-resistant *Staphylococcus aureus* (MRSA), has become a major threat to global health. Zinc Oxide Quantum dots (ZnO-QDs) show good antibacterial activity, but most of them are insoluble in water, limiting their application range, and there is a lack of research on drug resistance inducement.

Methods: The water-soluble zinc oxide quantum dots modified by APTES (ZnO@APTES QDs) were prepared by a microwave assisted synthesis. Then ZnO@APTES QDs were characterized through various methods. After confirmation of synthesized ZnO@APTES QDs, its bactericidal effect on MRSA was detected through in vitro and in vivo experiments, and its mechanism of action was analyzed.

Results: Characterization analysis revealed that the ZnO@APTES QDs have a particle size of 5 nm. The minimum inhibitory concentrations (MIC) were determined to be 64 μg mL^{-1} for *Escherichia coli* (*E. coli*) and 32 μg mL^{-1} for MRSA. The ZnO@APTES QDs showed significant inhibition of MRSA biofilm formation and effectively disrupted mature biofilms. Notably, the ZnO@APTES QDs did not induce tolerance or resistance even after 30 days of repeated exposure, whereas antibiotics led to a rise in bacterial MIC within 3 days and a 60-fold increase after 30 days. Mechanistic analysis indicated that the positively charged quantum dots interact with bacterial surfaces, altering membrane fluidity. Once inside the bacteria, the ZnO@APTES QDs generate reactive oxygen species (ROS), causing DNA damage and bacterial cell death. Moreover, the ZnO@APTES QDs possessed good biocompatibility and demonstrated significant therapeutic efficacy against drug-resistant bacterial infections in both macrophage and mouse wound infection models.

Conclusion: In summary, we have synthesized a highly effective water-soluble ZnO@APTES QDs that shows strong antibacterial and therapeutic efficacy against MRSA and other bacteria. The ZnO@APTES QDs holds significant potential for development as a new treatment agent for combating antibiotic-resistant infections.

Keywords: water-soluble, antibiotic resistance, biofilm, reactive oxygen species, wound

Introduction

Antibiotics have significantly contributed to saving human lives from bacterial infection in recent decades. However, the extensive use of antibiotics has resulted in the emergence of numerous multidrug-resistant (MDR) bacterial strains,

Received: 6 October 2024
Accepted: 5 January 2025
Published: 13 January 2025

Graphical Abstract

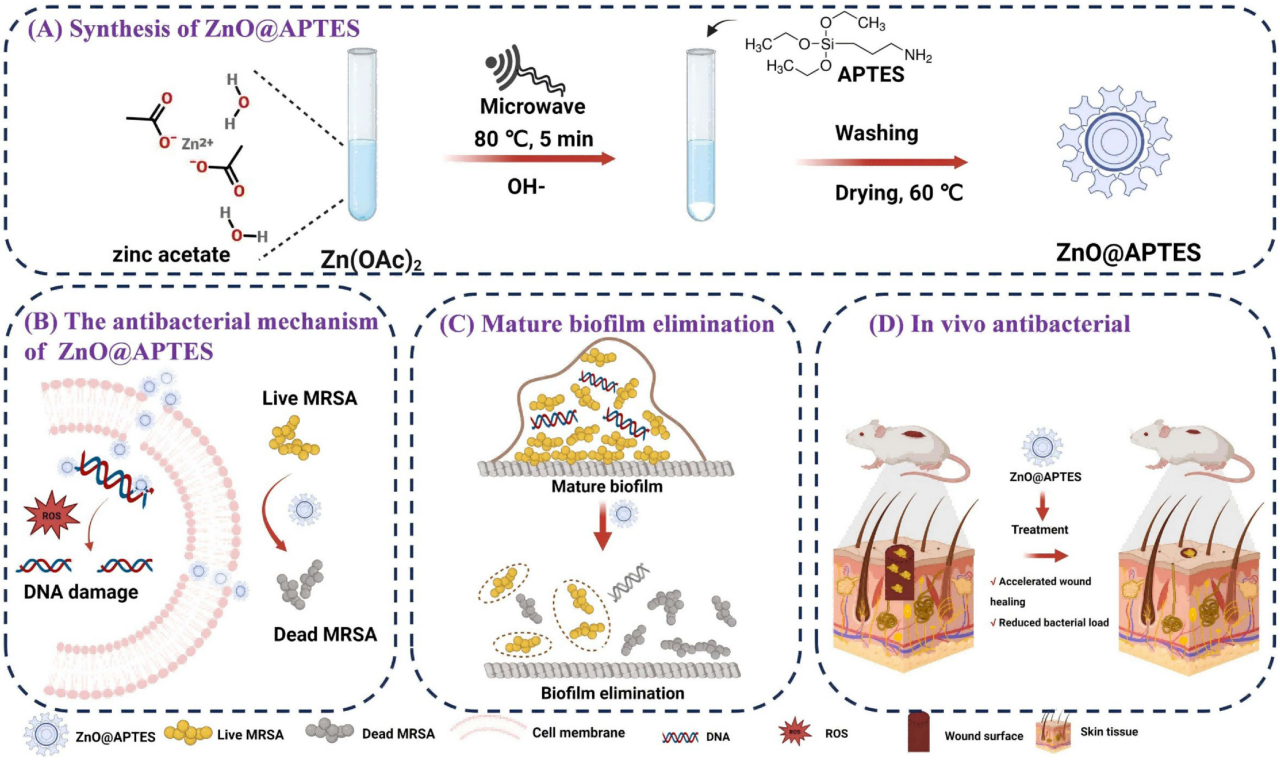

including the well-known "ESKAPE" superbugs such as MDR *Acinetobacter baumannii* (*A. baumannii*), MDR *Pseudomonas aeruginosa* (*P. aeruginosa*), MDR *Klebsiella pneumoniae* (*K. pneumoniae*), MDR *Enterobacteriaceae*, MDR *Staphylococcus aureus* (*S. aureus*), and vancomycin-resistant *Enterococcus faecium* (VRE). This has become a major public health crisis globally.[1,2] Antibiotic resistance was directly caused 1.27 million deaths in 2019, and an additional 4.95 million deaths were related to it. It is estimated that the death toll could be as high as 10 million by 2050.[3] In some regions, as many as 90% of *S. aureus* infections are reported to be Methicillin-resistant *Staphylococcus aureus* (MRSA).[4] Studies have shown that *S. aureus* can evade the killing of drugs through a complex variety of drugs resistance mechanisms.[5] It can not only initiate Intrinsic resistance to antibiotics by changing outer membrane permeability, using chromosomal encoded efflux pumps and producing antibiotic modifying enzymes and hydrolases. In addition, the acquired resistance mechanism can also be activated through gene mutation and the acquisition of exogenous drug resistance genes, thereby affecting the sensitivity of bacteria to antibiotics.[6] Therefore, there is an urgent need to explore new antibacterial strategies, especially non-antibiotic treatments, such as nano biotics, bacteriophages, immunotherapy and antimicrobial peptides, to address infections caused by MRSA.[7]

In the past few years, there has been a growing focus on exploring alternatives to antibiotics, where quantum dots (QDs) offer a promising therapeutic strategy for addressing antibiotic resistance due to their antimicrobial properties.[8] The nanoscale structure of zinc oxide QDs (ZnO-QDs) gives them unique advantages. Their particle sizes are usually 2–10 nm, which are far smaller than the cell diameters of most pathogenic microorganisms (usually 200–1000 nm), enabling it to easily penetrate the cell walls and cell membranes of bacteria, fungi and other microorganisms, directly into the cell interior for destruction.[9] Meanwhile, ZnO QDs has strong oxidation and can generate a large number of reactive oxygen species, which is one of the bactericidal mechanisms.[10] Furthermore, ZnO QDs have the abilities to disrupt cell membranes, interfere with specific metabolic pathways, and cause damage to DNA, all contributing to their bactericidal effect.[11]

ZnO QDs can be synthesized through chemical precipitation, hydrothermal, sol-gel methods using acetate precursors, and ultrasonic chemical synthesis.[12] The integration of microwaves with specific methods has garnered significant attention in materials science due to its rapid volumetric heating, shortened reaction time, minimized side reactions, enhanced reaction selectivity, energy efficiency, and improved production efficiency. Studies indicate that the antibacterial efficacy of nanomaterials is closely linked to their dispersion in water, with better dispersion resulting in enhanced antibacterial activity. The limited availability of synthesis methods for water-soluble QDs and the scarce antibacterial applications of existing water-soluble QDs have prompted the exploration of a novel water-soluble ZnO QDs for antibiotic resistance.[13]

In this study, we employed a microwave-assisted hydrothermal method to synthesize and modify ZnO QDs with (3-aminopropyl) triethoxysilane (APTES), generating water-soluble ZnO@APTES QDs. The resulting ZnO@APTES QDs showed potent antibacterial properties against MRSA without induction of resistance. These antibacterial effects were primarily due to the disruption of DNA and bacterial cell membranes by the Reactive oxygen species (ROS) generated by the ZnO@APTES QDs. Furthermore, the ZnO@APTES QDs exhibited limited cytotoxicity and hemolytic activity towards mammalian cells, and significant therapeutic efficacy against drug-resistant bacterial infections in both macrophage and mouse infection models.

Materials and Methods

Materials

Zinc acetate dihydrate (Zn $(CH_3COO)_2{\cdot}2H_2O$ 99.9%), potassium hydroxide (KOH 95%), APTES (99%), 8-Anilino-1-naphthalenesulfonate (ANS), 3-(4,5)-dimethylthiahiazo (-z-y1)-3,5-di- phenytetrazoliumromide (MTT), and glutaraldehyde (25% in H_2O) were obtained from Macklin, China. Ethanol anhydrous (99.7%) and sodium chloride (99.5%) were provided by Xilong Scientific, China. Yeast extract and tryptone were purchased from Oxoid (UK), phosphate-buffered saline (PBS) from Coolaber, China. LIVE/DEAD BacLight Bacterial Viability Kits were purchased from Invitrogen, USA. Dihydroethidium was obtained from Beyotime, China.2',7'-Dichlorodihydrofluorescein diacetate (DCFH-DA) was purchased from MedChemExpress, China. Bacterial DNA Genome Kit was purchased from Sangon, China. All other chemicals were of analytical grade. RAW 264.7 cell was obtained from Servicebio, China.

Microorganisms, Media, and Growth Conditions

Escherichia coli (E. coli) ATCC25922, *S. aureus* ATCC25923, MRSA ATCC43300 were purchased from Shanghai Luwei Technology Co., Ltd. Clinical strains such as MDR *S. aureus*, MDR *K. pneumoniae*, MDR *A. baumannii* and MDR *P. aeruginosa* were provided by the Wangjing Hospital, Chinese Academy of Chinese Medical Science. Their clinical code are shown in Table 1. MRSA ATCC43300 was cultured on soybean-casein digest agar medium (Trypticase soy agar [TSA]) and in Trypticase soy broth (TSB) at 37°C; the other bacteria were cultured in Mueller-Hinton broth (MHB) and on nutrient agar plates at 37°C.

Ethics Approval

Specific pathogen-free mice (ICR, female 6–8 weeks) were obtained from the Liaoning Experimental Animal Resource Center (Shenyang, China). All experiments were approved by the Laboratory Animal Management Committee of Shenyang Agriculture University (protocol: 20230511003) and were performed in compliance with the ethical guidelines for laboratory animals in China (GB/T 35892–2018 and GB/T 35823–2018).

Microwave-Assisted Synthesis and Characterization of ZnO@APTES Quantum Dots

ZnO@APTES QDs were synthesized using a microwave-assisted hydrothermal method, referring to previous synthesis methods with a novel modifications.[14] Briefly, $Zn(CH3COO)_2{\cdot}2H_2O$ was prepared as an aqueous solution at a concentration of 0.2 mol L^{-1} KOH was used as the alkali source and configured as an aqueous solution with a concentration of 0.5 mol L^{-1}. The alkaline solution was added to the precursor solution in a zinc-to-alkali molar ratio of 1:1 and microwaved to 80 °C for 5 min. Subsequently, 2 mL of a 20% APTES aqueous solution was added,

 https://doi.org/10.2147/IJN.S498672

Table 1 MIC of ZnO@APTES and LEV Against Gram-Negative Bacteria and Gram-Positive Bacteria

Strain	Identification Number	ZnO@APTES (μg mL^{-1})	Levofloxacin (μg mL^{-1})	Levofloxacin Susceptibility
E. coli	ATCC25922	64	0.5	Sensitive
S. aureus	ATCC25923	32	0.25	Sensitive
MRSA	ATCC43300	32	0.25	Sensitive
MDR *S. aureus*	22110608	32	4	Resistant
	22062928	32	4	Resistant
MDR *K. pneumoniae*	22062812	256	0.125	Sensitive
	22042909	128	128	Resistant
MDR *A. baumannii*	22063020	256	0.25	Sensitive
	23021703	128	16	Resistant
MDR *P. aeruginosa*	22050420	256	4	Resistant

Abbreviations: *E. coli, Escherichia coli. S. aureus, Staphylococcus aureus*. MRSA, Methicillin-Resistant *Staphylococcus aureus*. MDR, Multidrug-resistant. *K. pneumoniae, Klebsiella pneumoniae. A. baumannii, Acinetobacter baumannii. P. aeruginosa, Pseudomonas aeruginosa.*

resulting in the formation of a white precipitate. The white precipitate was washed with anhydrous ethanol and dried in an oven at 60 °C to obtain ZnO@APTES QDs.

The ZnO@APTES QDs were dissolved in water at a concentration of 1 mg mL^{-1}, and the resulting solution was observed under laser pointer and ultraviolet lamp irradiation. The water solubility of ZnO@APTES QDs was analyzed using a UV-visible spectrophotometer (Thermo Fisher Scientific, US), with a water dispersion of ZnO nanoparticles prepared in the laboratory as a control. The ZnO@APTES QDs were characterized using transmission electron microscopy (TEM, JEOL F200, Japan), X-ray diffraction (XRD, Bruker D8 Advance, Germany), X-ray photoelectron spectroscopy (XPS, Thermo Fisher Scientific, US), and Fourier transform infrared spectroscopy (FTIR, Shimadzu, Japan).

Antimicrobial Activity Test

MIC and MBC Test

The minimum inhibitory concentration (MIC) and minimum bactericidal concentration (MBC) tests were performed according to the research method of Wiegand.[15] MIC test was performed for all strains. The standard strains *E. coli* ATCC25922, *S. aureus* ATCC25923, MRSA ATCC43300 were tested for MBC. MIC and MBC were determined using the 96-well microtiter plate method. The experiment involved eight concentrations with separate groups for antibiotic control and negative control, each with three parallel batches. A bacterial suspension with a total concentration of 2.0×10^5 CFU mL^{-1} was added to the wells of a sterile 96-well plate, followed by different concentrations of ZnO@APTES QDs (final concentrations: 1024, 512, 256, 128, 64, 32, 16, 8, and 4 μg mL^{-1}) and antibiotics as controls. After incubation for 16–18 h at 37 °C, the MIC values were determined based on visible clarification of the mixed solution. Based on the MIC, 100 μL of the mixture was taken from the clarified well and plated on a non-resistant TSA plate or nutrient Agar plate at 37 °C overnight for culture. The MBC value was defined as the final concentration of ZnO@APTES QDs at which the number of bacterial colonies per 100μL volume was less than or equal to 5.

Bactericidal Kinetic Assay

To assess the changes in ZnO@APTES QDs activity over time, a bactericidal kinetic assay test was conducted. Optimizations were made based on Kumar's research method.[16] Bacterial suspensions with approximately 1.0×10^5 CFU mL^{-1} were exposed to varying concentrations of ZnO@APTES QDs in a shaking incubator (180 rpm) at 37 °C for

24 h. Viable colony counts were measured at different time points throughout the incubation period. Each assay condition was tested three times, and the average value was documented as the outcome.

Drug Resistance Induction

The induction of drug resistance was carried out following the research method of Hong.[17] MRSA ATCC 43300 was used as the model strains for resistance induction. Drug resistance was induced through repeated exposure of bacteria to sublethal doses (1/2 of MIC) of antimicrobial agents. The study involved testing ZnO@APTES QDs and levofloxacin (control) over a 30-day period against MRSA. The MIC was determined using the method described above. The bacteria were incubated in a culture medium with a sub-MIC concentration (1/2 of the MIC in that specific generation) for 24 h before being used for the subsequent MIC measurements. The development of drug resistance in MRSA was assessed by monitoring changes in MIC values normalized to the initial bacterial passage.

Biofilm Formation Inhibition Test

Biofilm formation inhibition and elimination tests were assessed by microtiter plates. [18] A 24-well plate was used to dilute a mixture of ZnO@ APTES QDs with varying concentrations by adding 2 mL of TSB. Simultaneously, each well was inoculated with a 1% volume fraction of MRSA at a concentration of 1.0×10^8 CFU mL^{-1} and then incubated at 37 °C for 48 h. After incubation, the suspension was discarded, and the wells were gently rinsed three times with sterile PBS. The wells were then fixed with methanol for 1 h, followed by another gentle rinse with sterile PBS. Subsequently, the wells were air-dried, and each well was stained with 2.1 mL of 1% crystal violet (w/v) for 10 min. After three rinses with ultrapure water, 2.1 mL of ethanol was used to dissolve the dye adhered to the biofilm cells. The absorbance of the dye-ethanol solution at 595 nm was measured using a microplate reader (BioTek, US).

In the laser confocal dish, ZnO@ APTES QDs and bacterial suspension were added according to the method described above, and incubated at 37 °C for 48 h. After incubation, the supernatant was discarded, and the dish was washed gently three times with PBS. The dead and live bacterial dye (LIVE/DEAD BacLight Bacterial Viability Kit, for microscopy and quantitative assays) was prepared by mixing 3 μL of each dye with 1 mL of physiological saline in a darkened centrifuge tube. The dye mixture was added to the central well of the laser confocal dish, protected from light, and incubated for 15–30 min. The stained coverslips were then rinsed twice with sterile PBS and observed using confocal laser scanning microscopy (CLSM, Leica, Germany).

Mature Biofilm Elimination Assay

In a 24-well plate, 2 mL of TSB was added to each well following a 1% volume fraction of 1.0×10^8 CFU mL^{-1} MRSA and incubated at 37 °C for 48h. Subsequently, the culture medium was removed, the wells were rinsed gently three times with PBS, and then 2 mL of TSB containing a mixture of ZnO@ APTES QDs with varying concentrations was added. After 4, 6, 8, and 24 h at 37 °C of incubation, the suspension was discarded, the plate was rinsed with sterile phosphoric acid and then gently washed three times with PBS. The samples were fixed with methanol for 1 h, followed by rinsing three times with sterile PBS, air drying, and staining of each well with 2.1 mL of 1% (w/v) crystal violet for 10 min. Then, they were rinsed three times with ultrapure water, and the dye attached to the biofilm cells was dissolved with 2.1 mL of ethanol. The absorbance of the dye-ethanol solution was measured at 595 nm using a microplate reader.

Mechanism of Antimicrobial Action of ZnO@ APTES QDs

Bacterial Morphological Characterization

The impact of ZnO@APTES QDs on MRSA was examined using a scanning electron microscope (SEM, Carl Zeiss AG, Germany). At 37 ° C, MRSA was incubated with ZnO@APTES QDs for 4h and centrifuged at 5000 rpm for 5 min to obtain bacteria. Then the bacteria fixed with 2.5% glutaraldehyde for 12 h, dehydrated with a series of ethanol concentrations (30%, 50%, 70%, 90%, and 100%), and imaged using SEM.

Zeta Potential Assay

The zeta potential of ZnO@ APTES QDs and bacteria were detected using a Zetasizer Nano Particle Analyzer (Malvern Instruments Ltd., UK).

Membrane Integrity Testing

ANS was used as a fluorescent probe to assess alterations in cell membrane fluidity.[19] A bacterial suspension in the logarithmic growth phase was washed thrice with PBS, resuspended, and adjusted to a concentration of 10^8 CFU mL^{-1}. The medicinal solution was added to achieve final concentrations of 4, 2.1, and 1/2 MIC in the bacterial suspension, with PBS used as a control. The suspension was incubated in a shaker at 37 °C for 12 h. Subsequently, the ANS fluorescent probe was introduced to the cell suspension at a final concentration of 4 μmol L^{-1} and incubated for 15 min at 37 °C in the absence of light. Fluorescence intensity was measured using a microplate reader with an excitation wavelength of 385 nm and an emission wavelength of 473 nm.

DNA Damage

A bacterial suspension in the logarithmic growth phase was resuspended and adjusted to a concentration of 10^8 CFU mL^{-1}. The medicinal solution was added to achieve final concentrations of 16 (1/2 MIC), 32 (MIC), and 64 (2MIC) μg mL^{-1} in the bacterial suspension. A drug-free medium served as a blank and was cultured in a shaker at 37 °C for 12 h. Total nucleic acids were extracted using the Bacterial DNA Genome Kit following the provided instructions.

Reactive Oxygen Species Detection

Bacterial cells at a concentration of approximately 1.0×10^8 CFU mL^{-1} were exposed to ZnO@ APTES QDs at 37 °C for 12 h. The ROS assay kit was utilized following the manufacturer's instructions. The bacterial samples were combined with 10 μM of DCFH-DA and incubated in the dark at room temperature for 1 h. The fluorescence intensity of the solution was then measured using a microplate reader with excitation/emission wavelengths set at 488/525 nm.

Determination of Superoxide in Bacteria

The possibility of superoxide anion (O_2^-) production was evaluated to determine oxidative stress using a superoxide assay kit. Briefly, 200 μL of the bacterial suspension was centrifuged and washed twice with sterile water, followed by the addition of 200 μL of detection solution and incubation at 37 °C for 5–10 min. Next, the bacterial samples were incubated with different concentrations of ZnO@ APTES QDs under the same conditions as described above. Finally, the samples were examined using a microplate absorbance reader at 450 nm.

Biocompatibility Test

MTT Assay

The MTT tetrazolium assay is a popular tool in estimating the metabolic activity of living cells.[20] RAW 264.7 cells were cultured in a sterile 96-well microtiter plate for 12 h, followed by treatment with varying concentrations of ZnO@APTES QDs in the culture medium at 37 °C (5% CO_2) for an additional 12 h. Subsequently, 10 μL of MTT solution (5 mg mL^{-1}) was added to each well and incubated for 4 h. After removing the cell supernatant, 150 μL of DMSO was added, and the plate was gently shaken for 10 min. The absorbance of the resulting solution at 490 nm (A490) was measured using a microplate reader. The cell viability percentage was calculated following formula:

$$Cell\ viability(\%) = \frac{A(experimental\ group) - A(blank\ group)}{A(negative\ control\ group) - A(blank\ group)}$$

Hemolysis Test

Red blood cells were isolated from mouse blood using a previously described method.[21] They were centrifuged at 2000 rpm for 15 min, washed three times with normal saline, and resuspended in normal saline to create a red blood cell suspension with a hematocrit of 2%. Varying concentrations of ZnO@APTES QDs were incubated with the 2% isovolumetric red blood cell suspension at 37 °C for 2 h. Triton X-100 (1%) and normal saline were employed as controls. Following incubation, the supernatant was collected, centrifuged at 3000 rpm for 5 min, and transferred to a 96-

well plate for analysis. The absorbance of the supernatant was measured at 450 nm (A450). The hemolysis rate was calculated following formula:

$$Hemolysis\ ratio(\%) = \frac{A(experimental\ group) - A(negative\ control\ group)}{A(positive\ control\ group) - A(negative\ control\ group)}$$

Treatment for Macrophage Infection Model

Macrophage infection model was prepared by improving on the basis of previous studies.[22] An infection model of RAW 264.7 macrophages infected with MRSA was established to evaluate the antibacterial ability of ZnO@ APTES QDs in macrophages. Macrophages were infected with MRSA at a multiplicity of infection (MOI) of 10:1 and incubated in an antibiotic-free medium at 37 °C for 2 h. After culture, the cells were centrifuged at 5000 rpm for 5 min and washed three times with sterile saline. RAW 264.7 cells were then incubated with medium containing 30 μg mL^{-1} of ZnO@ APTES QDs for 2 h. Levofloxacin treatment was used as the control group. To quantify the drug efficacy, 100 μL of diluted mixtures with and without ZnO@APTES QDs treatment were plated on TSA plates. The number of colonies was counted after incubation.

Treatment for Mice Skin Infection Model

The macrophage infection model was prepared by improving based on previous studies.[23] A mouse model of MRSA infection was prepared. Scalds were performed on the back skin of anesthetized mice with heated 1 cm^3 metal blocks, followed by subcutaneous injection of MRSA (1.0×10^9 CFU mL^{-1}) in 100 μL normal saline. After 2 days of infection, the wounds infected with MRSA (10^8 CFUs per wound) were treated with a single dose of ZnO@APTES QDs (3.6 mg kg^{-1}, 5 mg mL^{-1}). Positive control was administered with levofloxacin (0.1 mL, 5 mg mL^{-1}), and negative control with normal saline (NaCl, 0.9%). The wound size was monitored every 2 days, and the mice were killed on day 10. The infected tissues were homogenized, and colonies were cultured to evaluate the treatment efficacy.

Statistical Analysis

Statistical analysis was performed using GraphPad Prism 10 software (USA). All experiments were replicated three times, and a one-way ANOVA or Mann–Whitney test was employed to identify significant differences between samples. The results were presented as mean ± standard deviation. $P < 0.05$ was considered statistically significant.

Results

Synthesis and Characterisation of ZnO@ APTES QDs

ZnO@ APTES QDs were synthesized using a microwave-assisted hydrothermal method in ethanol. The synthesized ZnO@ APTES QDs were then characterized with different techniques. The results, depicted in Figure 1A, demonstrate that ZnO@APTES QDs can be easily dissolved in water. Laser pointer penetration observation revealed the Tyndall effect in water, indicating its dispersion into a colloidal solution. When exposed to ultraviolet light, the solution exhibited a yellow color and fluorescence. Additionally, Figure 1B illustrates that the transmittance of the ZnO@APTES QDs solution under ultraviolet and visible light exceeded 98%, whereas the unmodified ZnO control exhibited a maximum transmittance of only 20%. These findings suggest that ZnO has enhanced the water solubility post-modification.

The TEM image in Figure 1C shows that the ZnO@APTES QDs particles are almost uniform. Image J (National Institutes of Health, USA) was used to measure 100 random particle diameters and create a particle size distribution map, and the particle size was approximately 5nm (Figure 1D). The XRD spectrum of ZnO@APTES QDs (Figure 1E) displayed peaks consistent with the hexagonal wurtzite structure, indicating phase purity without additional impurity peaks. The broad peaks observed align with the synthesis of small-sized ZnO QDs.[24] ZnO@APTES QDs exhibit XRD patterns similar to uncoated ZnO nanoparticles, suggesting that the crystal structure remains unaffected by the surface coating.

To verify the successful coating of silane on the ZnO@APTES QDs, XPS analyses were conducted. The results in Figure 1F show the presence of Zn (1021.1 eV), O (530.1 eV), N (399.9 eV), C (284.8 eV), and Si (101.85 eV) on the

https://doi.org/10.2147/IJN.S498672

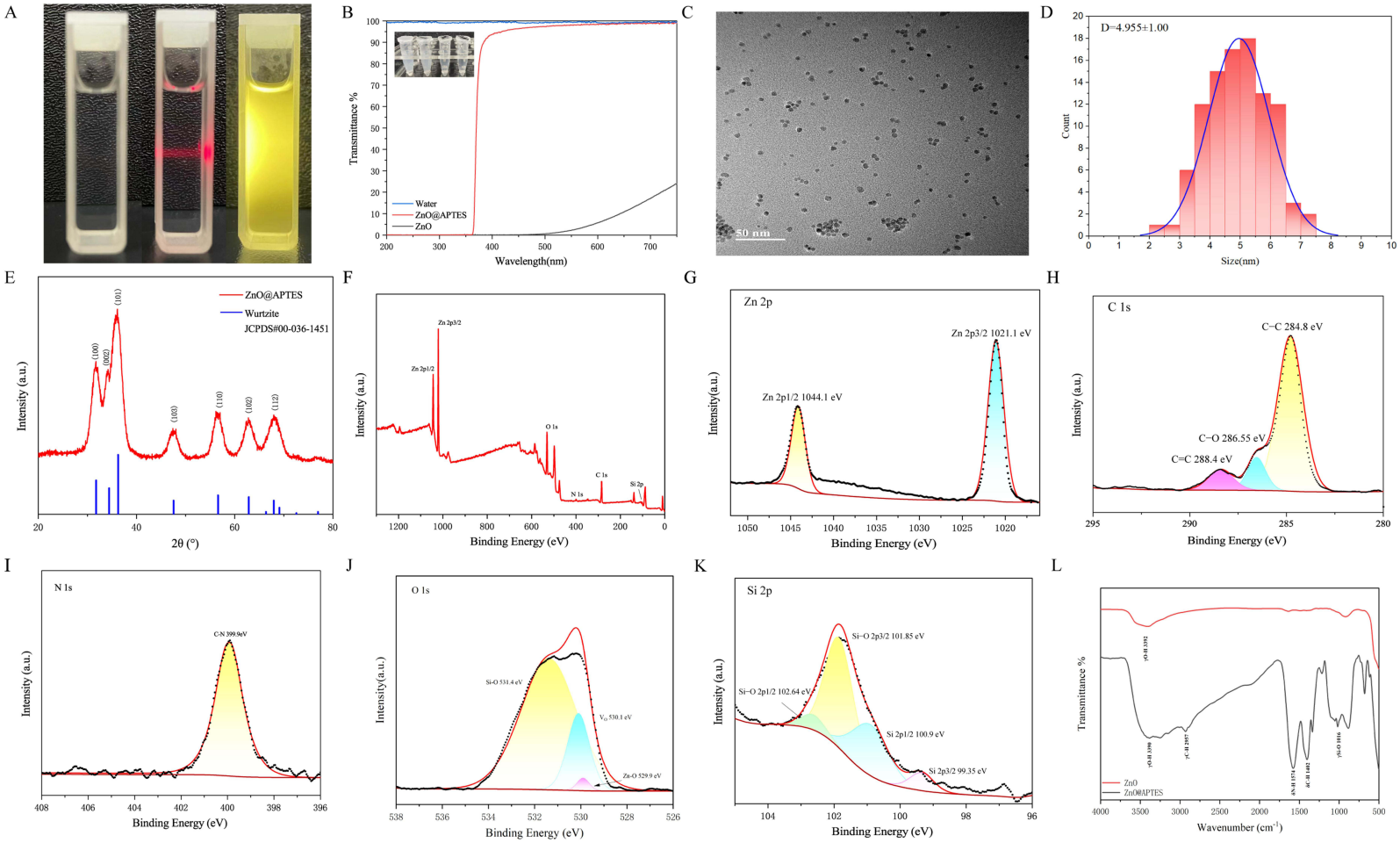

Figure 1 Characterization results of ZnO@APTES QDs: (**A**) Raw liquid appearance, Tyndall effect, and color under ultraviolet light exposure. (**B**) Water solubility detection, (**C**) TEM image, (**D**) Histogram of particle size, (**E**) XRD, (**F**) XPS elemental distribution, (**G**)-K) High-resolution XPS spectra of: Zn 2p (**G**), C 1s (**H**), N 1s (**I**), O 1s (**J**), and Si 2p (**K**), (**L**) FTIR.

Abbreviations: ZnO@APTES QDs, water-soluble APTES modified zinc oxide quantum dots.

surface of the QDs. The high-resolution Zn 2p spectrum revealed peaks at 1021.1 and 1044.1 eV (Figure 1G), whereas peaks at 288.4, 286.55, and 284.8 eV were attributed to C=C, C-O, and C-C, respectively (Figure 1H). In the QDs, a single peak at 399.9 eV was assigned to C-N (Figure 1I). Deconvolution of the O 1s spectrum yielded peaks at 531.4, 530.1, and 529.9 eV (Figure 1J). The Si 2p spectrum displayed peaks at 102.64, 101.85, 100.9, and 99.35 eV, corresponding to different Si-O bonds (Figure 1K).

As shown in Figure 1L, the peaks of FTIR observed at 3390, 2957, 1574, 1402, and 1016 cm^{-1} correspond to the vibrations of O-H, C-H, N-H, C-H, and Si-O. These findings are in line with previous research.[14]

ZnO@ APTES QDs is Effective for Both Sensitive and Resistant Superbugs

The broth dilution method was used to determine the MIC to study the antibacterial activity of ZnO@APTES QDs. First, antibiotic-sensitive strains of *E. coli* ATCC25922, *S. aureus* ATCC25923 and MRSA ATCC43300 were selected as bacterial models to test the ZnO@APTES QDs antibacterial ability. ZnO@APTES QDs have antibacterial activity against these representative strains, with an MIC range of 32–64 μg mL^{-1} and an MBC range of 256–64 μg mL^{-1} as shown in Figure 2A, suggesting that ZnO@APTES QDs may have broad-spectrum antibacterial properties. The results of this study showed that gram-positive bacteria were more sensitive to ZnO@APTES QDs than gram-positive bacteria, which was consistent with previous results.[25] Additionally, the effects of ZnO@APTES QDs on clinical isolates of ESKAPE strains (ie, MDR *A. baumannii*, MDR *P. aeruginosa*, MDR *S. aureus* and MDR *K. pneumoniae*) were evaluated. Levofloxacin was used as an antibiotic control group, but its antibacterial effect was not significant. In

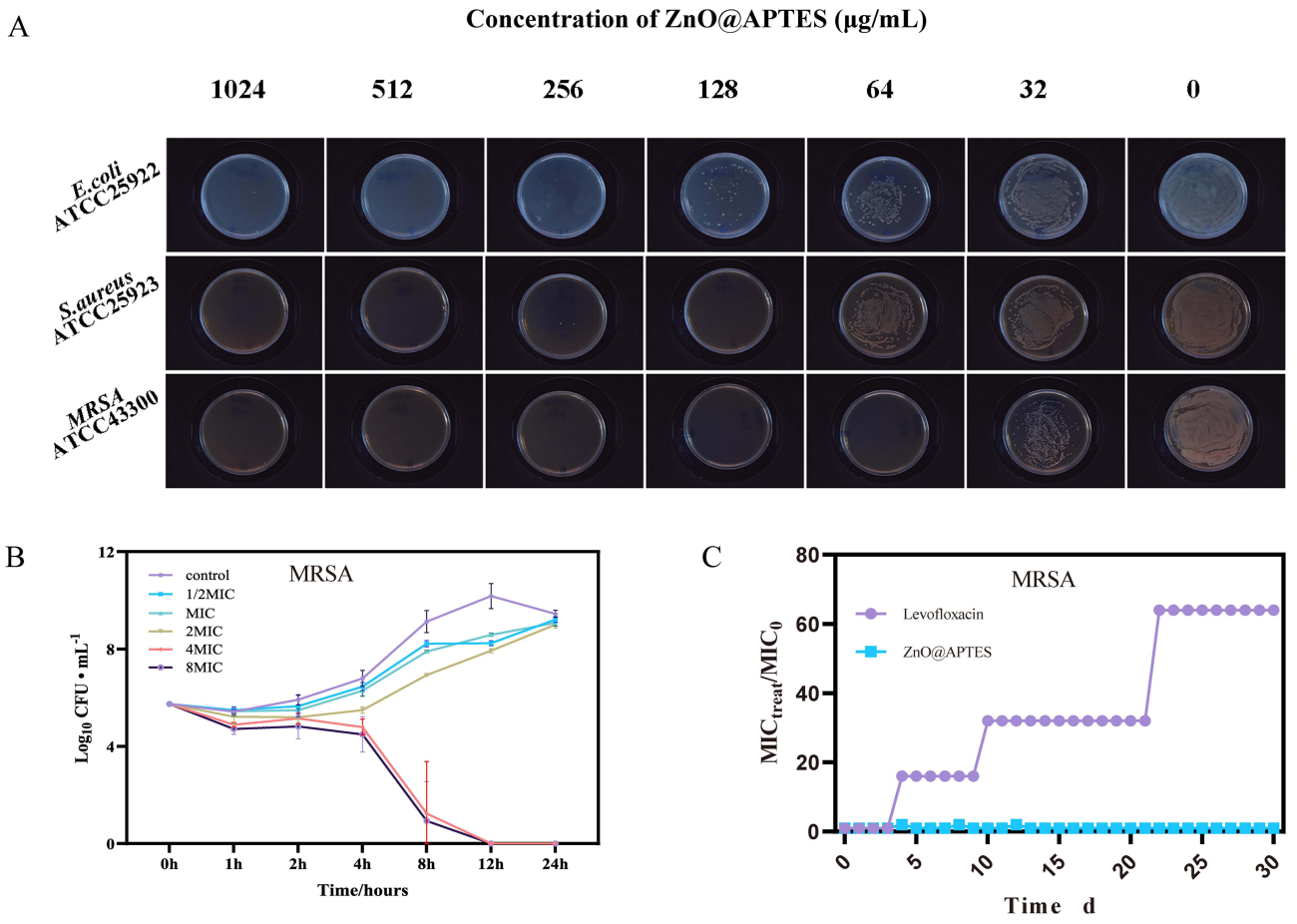

Figure 2 Antibacterial Activity of ZnO@APTES: (**A**) MBC against *E. coli, (S) aureus*, MRSA. (**B**) Bactericidal curve against MRSA. (**C**) Long-term bacterial resistance induction against MRSA.

Abbreviations: *E. coli, Escherichia coli; S. aureus, Staphylococcus aureus*; MRSA, Methicillin-Resistant *Staphylococcus aureus*; ZnO@APTES QDs, water-soluble APTES modified zinc oxide quantum dots; CFU, Colony-Forming Units; MIC, minimum inhibitory concentration.

https://doi.org/10.2147/IJN.S498672

contrast, ZnO@APTES inhibited the proliferation of MDR *S. aureus*, MDR *A. baumannii*, MDR *P. aeruginosa*, and MDR *K. pneumoniae*, with MICs of 32, 256–128, 256–128 and 256 μg mL^{-1} respectively (Table 1).

Killing kinetic analysis was performed to determine the changes in the activity of the ZnO@APTES over time. As shown in Figure 2B, the antibacterial behavior of ZnO@APTES against the test bacteria showed concentration and time dependence, with different dynamics against MRSA ATCC43300. ZnO@APTES caused a significant reduction in the number of MRSA ATCC43300 colonies within 8 h, and at 12 h at 4 × MIC concentration, all bacterial cells were eradicated. These data showed that ZnO@APTES QDs not only have high antibacterial activity against superbugs but also have rapid killing kinetics.

Long-Term Repeated Treatment with ZnO@APTES QDs Does Not Induce Tolerance and Resistance

Long-term bacterial resistance induction is a great challenge in current infection treatment.[26] The use of any new antibiotics invariably leads to the emergence of drug-resistant strains. To evaluate the potential bacterial resistance to ZnO@APTES QDs, a standard strain of MRSA was repeatedly exposed to ZnO@APTES QDs at sublethal concentrations (1/2 MIC). As expected, MRSA rapidly developed significant sublethal dose resistance to the conventional antibiotic levofloxacin within days (Figure 2C). The ratio of MIC_{treat} to MIC_0 in the levofloxacin induced group increased over 10 folds in 3 days, increased to 30 at 10^{th} and peaked at 60 at 22^{nd} during the 30 days period. However, no resistance to ZnO@APTES QDs developed even after 30 days of continuous treatment. The results showed that ZnO@APTES QDs is a new and effective antimicrobial agent that does not induce tolerance and resistance even after long-term treatment.

ZnO@APTES QDs is Highly Effective Against MRSA Biofilms

Bacterial biofilms are a significant contributor to persistent infections and can enhance drug resistance.[27] In this study, MRSA was utilized as a model to assess the impact of ZnO@APTES QDs on both biofilm formation and mature biofilms. Firstly, we evaluate its impact on biofilm formation. The results showed that ZnO@APTES QDs exhibited strong anti-biofilm activity, with even minimal concentrations effectively inhibiting MRSA biofilm formation (Figure 3A). As shown in Figure 3B, the introduction of ZnO@APTES QDs led to a reduction in the thickness and density of bacterial biofilms, suggesting that ZnO@APTES QDs have inhibitory effects on biofilm formation. Then, we analyzed the impact of ZnO@APTES QDs on mature biofilms. The elimination experiment results of mature biofilms are shown in Figure 3C, where the better the biofilm removal effect is with the increase of drug concentration and the longer the drug action time, which is consistent with the results of the bactericidal kinetic curve. Figure 3D showed the action of ZnO@APTES QDs on mature biofilms.

Antibacterial Mechanism of ZnO@APTES QDs Against MRSA

The antibacterial mechanism of ZnO@APTES QDs was investigated using MRSA as model. Scanning electron microscopy (SEM) was utilized to further validate this mechanism. Untreated MRSA exhibited intact and smooth morphology (Figure 4A). However, exposure to 32 ug mL^{-1} ZnO@APTES QDs for 2 h at 37°C resulted in shrunken and damaged MRSA cells (Figure 4A). These findings support the notion that ZnO@APTES QDs effectively interacts with MRSA membranes, leading to cell damage and ultimately killing the superbugs.[28]

In this study, as shown in Figure 4B, the zeta potentials of ZnO@APTES QDs and bacteria are completely opposite, with the absolute potential values of Gram-positive bacteria higher than those of Gram-negative bacteria.

To investigate the impact of ZnO@APTES QDs on bacterial cell membranes, the ANS method was employed to assess membrane integrity. The ANS contains a non-polar benzene ring that binds to membrane lipids at the lipid-water interface. Changes in its fluorescence intensity indicate alterations in the environment of the membrane lipid binding site. The fluorescence quantum yield of ANS correlates with the fluidity of the membrane lipid polar region: a smaller fluorescence intensity value indicates higher fluidity, while a larger value suggests lower fluidity.[29] The results in Figure 4C reveal that MRSA cell membranes co-incubated with ZnO@APTES QDs exhibited binding to ANS, with

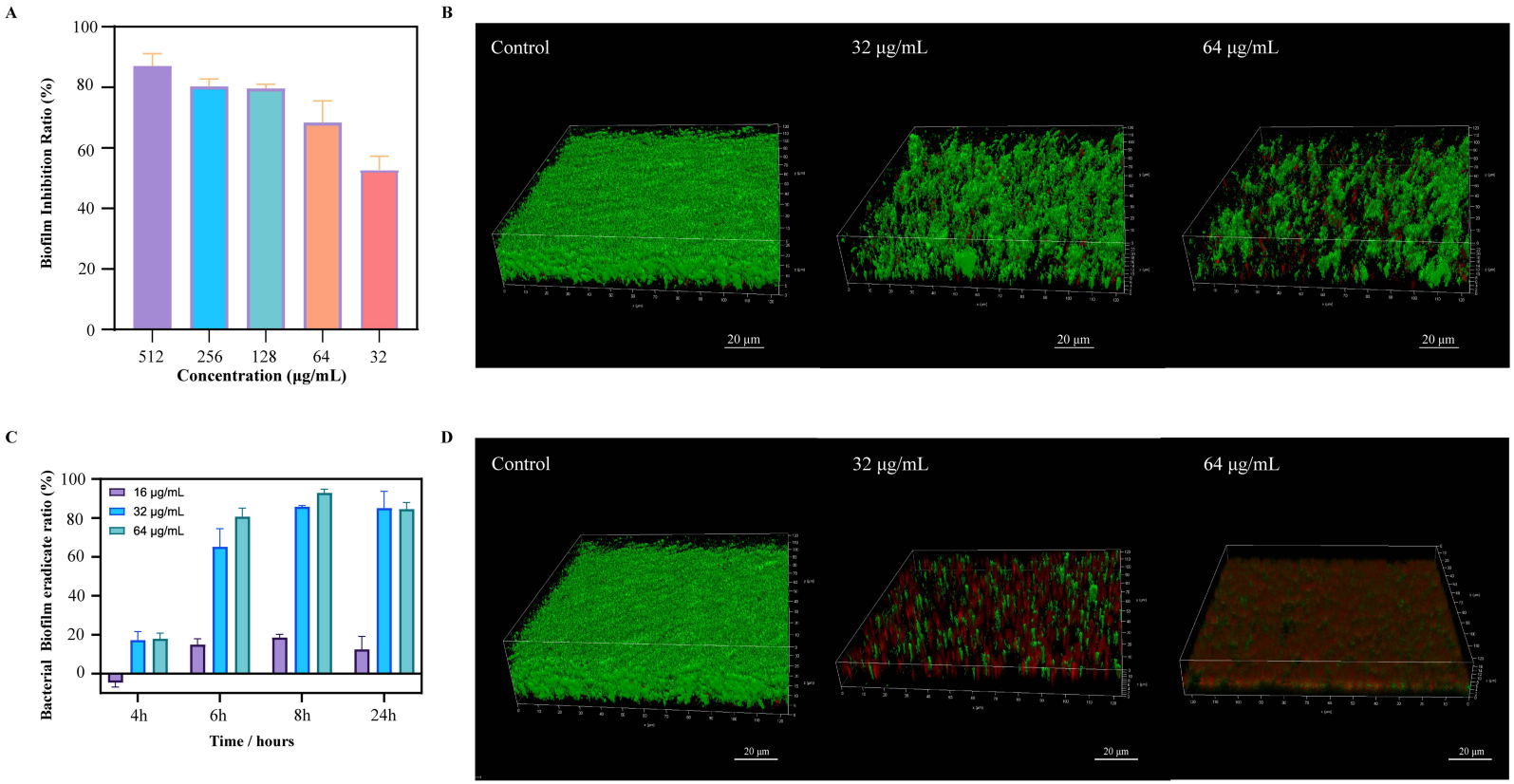

Figure 3 Inhibition and elimination of MRSA biofilm by ZnO@APTES QDs: (**A**) Inhibition of biofilm by different concentration of ZnO@APTES QDs, (**B**) CLSM of biofilm formation inhibition by ZnO@APTES QDs, (**C**) Elimination effect on the mature biofilm by ZnO@APTES QDs under different drug concentrations and action times, (**D**) CLSM of biofilm elimination by ZnO@APTES QDs.
Abbreviations: ZnO@APTES QDs, water-soluble APTES modified zinc oxide quantum dots; MIC, minimum inhibitory concentration; CLSM, confocal laser scanning microscopy.

https://doi.org/10.2147/IJN.S498672

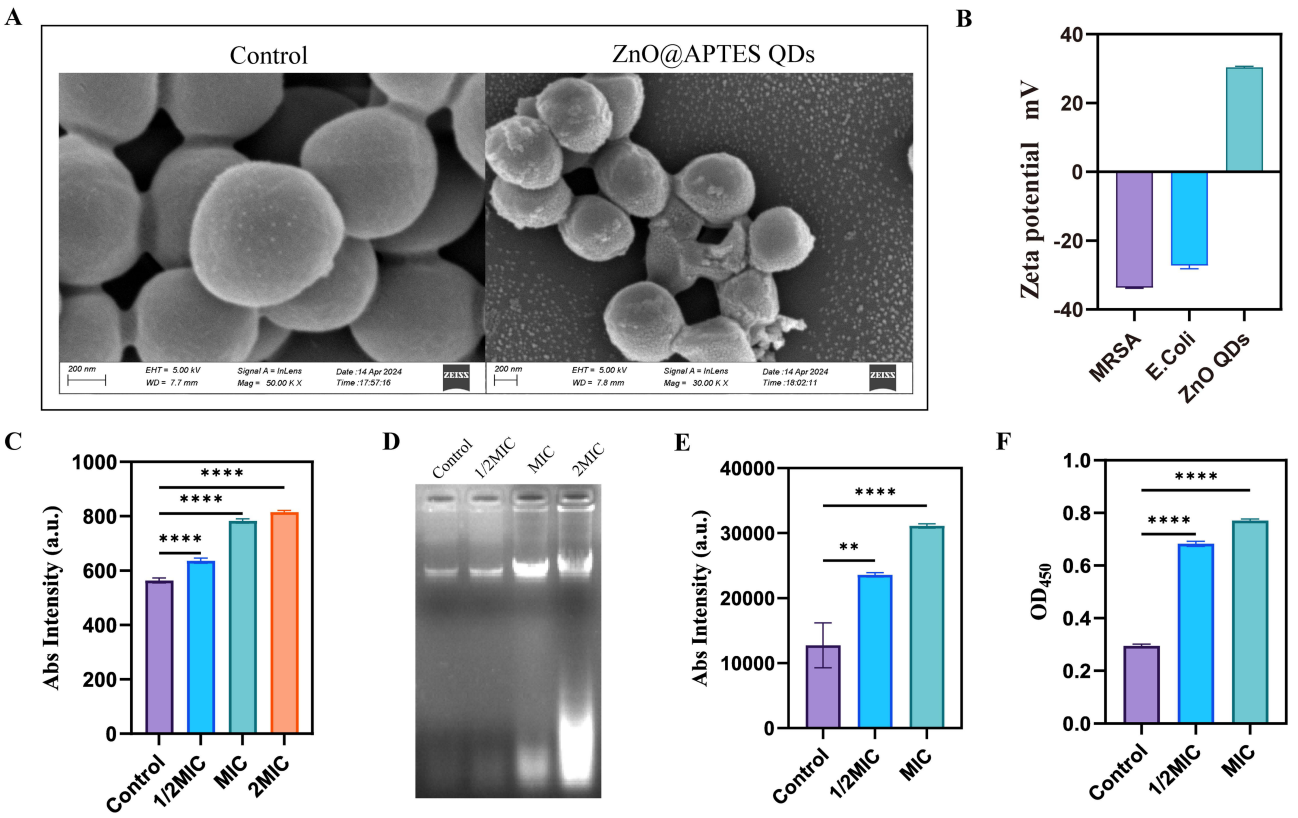

Figure 4 Bacteriostatic Mechanisms of ZnO@APTES QDs on MRSA: (**A**) Scanning electron micrographs after administration, (**B**) Zeta potential of ZnO@APTES QDs and bacteria, (**C**) Disruptive effects of bacterial membranes by ZnO@APTES QDs at different concentrations, (**D**) DNA damage, (**E**) Total ROS production in the bacterium, (**F**) Superoxide (O_2^-) production of the bacteria at different concentrations of ZnO@APTES QDs.

Notes:**: p≤0.01, ****: p≤0.0001.

Abbreviations: ZnO@APTES QDs, water-soluble APTES modified zinc oxide quantum dots; MIC, minimum inhibitory concentration; Abs, absorbency; *E. coli, Escherichia coli*; MRSA, Methicillin-Resistant *Staphylococcus Aureus*; OD, Optical Density.

the binding intensity increasing as the concentration of ZnO@APTES QDs rises. This suggests that the antibacterial efficacy of ZnO@APTES QDs is contingent upon concentration.

Following extensive cell membrane destruction, ZnO@APTES QDs can readily penetrate bacteria and interact with bacterial genomic DNA, leading to DNA damage either directly or indirectly. To validate this phenomenon, the genomic DNA of bacteria exposed to ZnO@APTES QDs was isolated and subjected to electrophoretic analysis. As shown in Figure 4D, both untreated and 1/2MIC-treated MRSA samples exhibited dense DNA bands, suggesting an absence of DNA damage. In contrast, the DNA bands of the 1 and 2 MIC treated group displayed noticeable after-swells, indicating the occurrence of DNA fragment shortening and genomic DNA damage.

We investigated the antibacterial efficiency of ZnO@APTES QDs driven by ROS generation. As shown in Figure 4E, compared to the control group, the ZnO@APTES QDs treatment significantly induces intracellular ROS production in bacteria, and it increases with the increase of ZnO@APTES QDs concentration. Furthermore, to identify whether the cellular oxidative stress was induced by ZnO@APTES QDs, the ROS-dependent oxidative stress was investigated. The production of O_2^- at different ZnO@APTES QDs concentrations was monitored using the Superoxide Assay Kit. As shown in Figure 4F, the absorption values increased notably with an increasing ZnO@APTES QDs concentration, revealing that ZnO@APTES QDs mediated the superoxide anion production, which played an important role in the antibacterial activity.

ZnO@APTES QDs is Biocompatible and Safe

To preliminarily assess the biocompatibility of ZnO@APTES QDs with mammalian cells, MTT experiments were conducted using mouse macrophages RAW267.4 as a model. As shown in Figure 5A, the results indicated that even

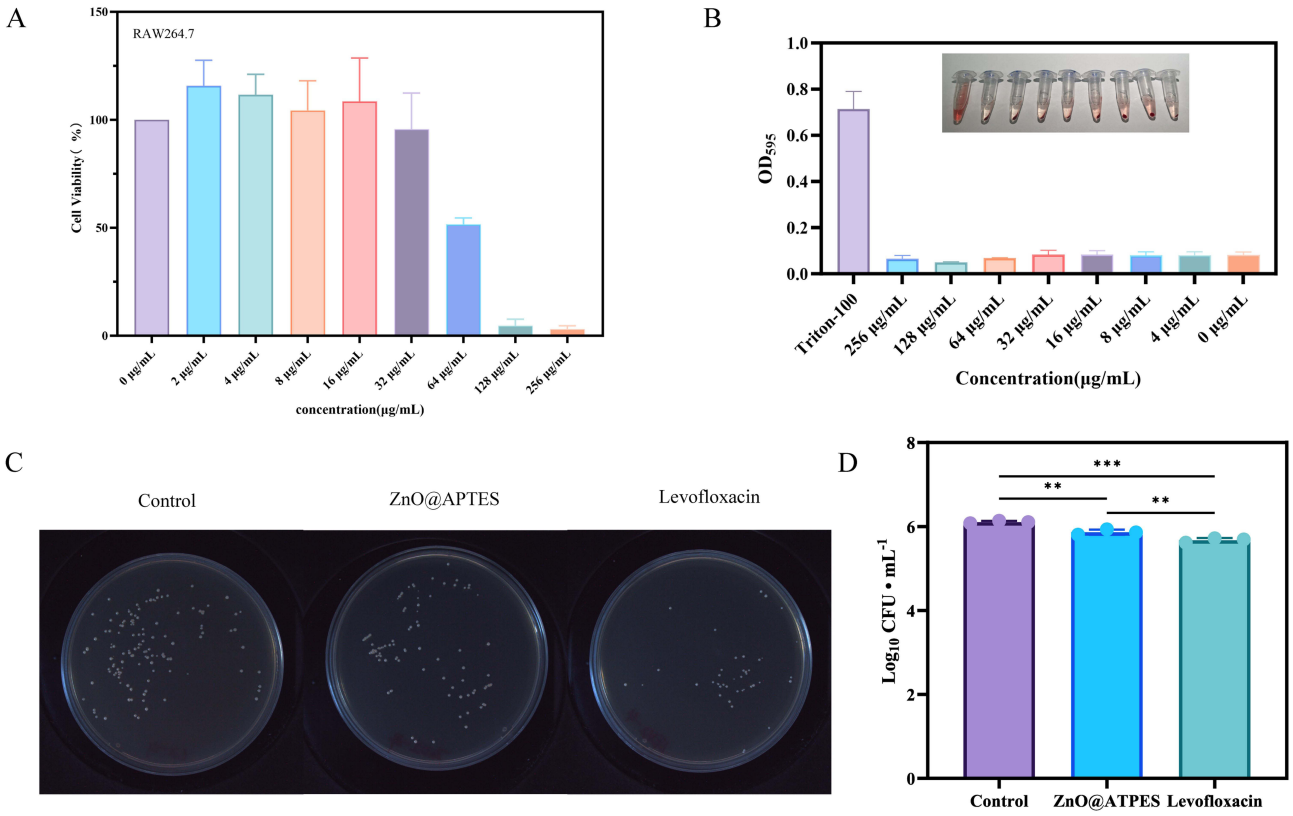

Figure 5 Biocompatibility evaluation. (**A**) Cell viability of RAW264.7 cells treated with different concentrations ZnO@APTES QDs, (**B**) The hemolysis of different concentrations ZnO@APTES QDs, (**C**) and (**D**) Photographs and corresponding statistics of MRSA colonies formed on LB agar plates after co-culturing with ZnO@APTES QDs; MRSA and RAW 264.7 macrophages.

Notes: **: p≤0.01, ***: p≤0.001.

Abbreviations: ZnO@APTES QDs, water-soluble APTES modified zinc oxide quantum dots; MRSA, Methicillin-Resistant Staphylococcus Aureus; OD, Optical Density; CFU, Colony-Forming Units.

at a high dose of 64 μg mL^{-1}, the survival rate of mouse macrophage RAW267.4 was 51.54%, surpassing the MIC of MRSA. The hemolytic behavior of mouse red blood cells treated with ZnO@APTES QDs showed no significant hemolysis at higher doses (Figure 5B). The results show that ZnO@APTES QDs have good biocompatibility with mammalian cells.

To further explore the potential of biocompatible ZnO@APTES QDs for applications, in vitro antibacterial efficacy was assessed using a co-culture model of MRSA bacteria and RAW 264.7 macrophages. The presence of ZnO@APTES QDs led to a significant reduction in intracellular MRSA compared to that of control group (Figure 5C and D). The number of MRSA colonies further confirmed the strong antibacterial activity of ZnO@APTES QDs against MRSA within macrophages. These findings clearly indicate that ZnO@APTES QDs can effectively eliminate superbugs within macrophages while maintaining good biocompatibility with the macrophages themselves.

Efficient Treatment of Challenging MRSA Wound with ZnO@APTES QDs

To assess the effectiveness of ZnO@APTES QDs against superbugs in vivo, a mouse skin infection model was utilized. Results indicated that after 10 days, wounds in the ZnO@APTES QDs group healed significantly, while the negative control group still exhibited a high wound size (Figure 6A and 6B). ZnO@APTES QDs and levofloxacin treatments accelerated wound healing and reduced infection risk. Bacterial load analysis revealed a substantial reduction of MRSA levels in mice treated with ZnO@APTES QDs compared to those with saline treatment, showing a bactericidal effect of 99% (Figure 6C).

https://doi.org/10.2147/IJN.S498672

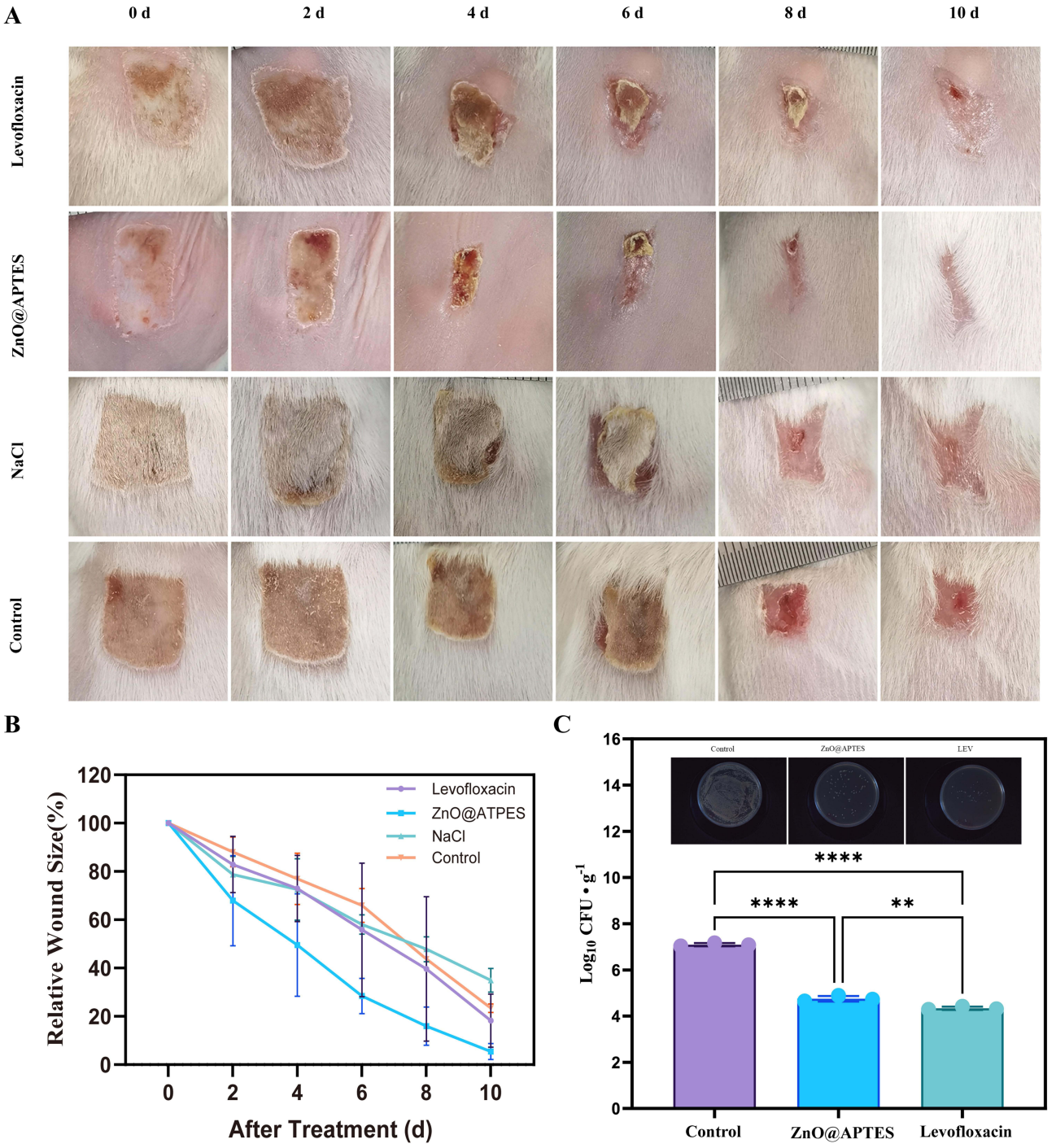

Figure 6 Therapeutic effect of ZnO@APTES QDs on mouse skin infection model: (**A**) Representative photographs of untreated and MRSA-infected wounds treated with ZnO@APTES QDs, (**B**) Corresponding wound size (relative area vs initial area), (**C**) Photographs of colony formation on TSA of homogenized tissue dispersions from infected sites of mice injected with ZnO@APTES QDs (10 d), Saline (NaCl, 0.9%) and levofloxacin (0.1 mL, 5 mg mL^{-1}) were used as negative and positive controls for testing.
Notes: **: p≤0.01, ****: p≤0.0001.
Abbreviations: ZnO@APTES QDs, water-soluble APTES modified zinc oxide quantum dots; MRSA, Methicillin-Resistant Staphylococcus Aureus; CFU, Colony-Forming Units.

Discussion

Infections caused by MRSA pose a serious threat to public health, making the development of new antimicrobial agents to combat multidrug-resistant infections critically important.[30,31] Some novel QDs antimicrobial agents, such as ZnO QDs, have garnered widespread attention due to its excellent properties, including good antibacterial activity, low cost,

and simple preparation.[32,33] Previous studies have shown that nano-zinc oxide exhibits good antibacterial activity against MRSA, but it currently faces issues such as poor water solubility and low biocompatibility.[34] Therefore, in this study, to overcome the limitations of ZnO and enhance its antibacterial properties, we synthesized ZnO@APTES QDs using a microwave-assisted method. ZnO@APTES QDs possess excellent antibacterial activity without inducing resistance, and they also exhibit good water solubility and biocompatibility.

Microwave-assisted synthesis is one of the latest techniques for preparing QDs.[35] It can accelerate chemical reactions through microwave heating, thereby improving the synthesis efficiency and yield of QDs. In this study, ZnO@APTES QDs were synthesized in ethanol using a microwave-assisted hydrothermal method. The results showed that the solution prepared by this method exhibited yellow fluorescence under UV light, which is a unique property of the QDs.[36] APTES is one of the most important silicon compounds in chemistry for the synthesis of materials. It has been widely used as a silanization agent for the chemical modification of metal oxide nanoparticle surfaces.[37] Therefore, after modification with APTES, its water solubility is significantly enhanced. Subsequent characterization results showed that the ZnO@APTES QDs prepared by this method are consistent with those synthesized by the conventional hydrothermal method, both exhibiting the typical characteristics of ZnO QDs.[38]

In vitro antibacterial tests showed that ZnO@APTES QDs exhibit good killing activity against both standard strains and clinical isolates of MRSA. The results of this study are consistent with previous reports on the antimicrobial properties of ZnO nanoparticles.[39] Simultaneously, long-term use does not induce the development of resistance. Since this material primarily exerts its antibacterial effect by directly physically disrupting the bacterial structure, without relying on chemical reactions or antibiotics, it effectively avoids the resistance issues that may arise with traditional antimicrobial agents.

Infections caused by MRSA after biofilm formation are characterized by strong environmental adaptability, a high tendency to develop resistance, and difficulty in being cleared by the host immune system.[40] As a result, it is challenging to find suitable treatment options, which poses a serious threat to human health and leads to significant economic losses. Therefore, the removal of MRSA biofilms is also key to preventing the formation of resistance.[41] This study shows that ZnO@APTES QDs significantly inhibit the formation of MRSA biofilms and can also remove mature biofilms. These findings align with previous research on organometallic materials inhibiting MRSA biofilms, underscoring the promising anti-biofilm properties of ZnO@APTES QDs.[42,43]

Further research on the antibacterial mechanism show that the antibacterial effect of ZnO@APTES QDs primarily relies on quantum tunneling effects, electrostatic interactions, DNA damage, and oxidative stress. ZnO@APTES QDs can physically penetrate the cell wall through quantum tunneling effects, leading to mechanical damage to MRSA. The opposite zeta potentials of nanomaterials and bacteria facilitate their electrostatic interactions at the bacterial membrane surface, thereby enhancing the antibacterial activity of nanomaterials.[44,45] Our result indicates a strong electrostatic interactions between ZnO@APTES QDs and bacteria, with Gram-positive bacteria showing higher interaction with ZnO@APTES QDs compared to that of Gram-negative bacteria. This also explains why ZnO@APTES QDs exhibit better bactericidal efficacy against Gram-positive bacteria than Gram–negative bacteria. The high positive charge on the surface of ZnO@APTES QDs facilitates this electrostatic adsorption, leading to efficient internalization by the bacteria. Due to electrostatic interactions, positively charged ZnO nanoparticles can easily attach to the bacterial cell membrane. This interaction can disrupt the membrane structure and compromise cell integrity, leading to bacterial death.[46] Simultaneously, ZnO@APTES QDs also cause cell membrane of MRSA damage. The cell membrane is a semipermeable membrane with selective permeability, composed of a phospholipid bilayer forming the basic framework. Its main components are proteins and lipids, with small amounts of carbohydrates.[47] The fluidity of the cell membrane is defined as the relative lateral movement of proteins and lipids within the membrane structure. Numerous vital cellular functions are closely linked to membrane fluidity. Loss of cell membrane fluidity disrupts normal bacterial activity. When ZnO@APTES QDs enter the MRSA, it can disrupt the bacterial metabolic activity, generate a large amount of ROS, and induce oxidative damage to the cell membrane. At the same time, it causes damage to bacterial protein synthesis and DNA replication, ultimately leading to the death of MRSA. It is a common mechanism of inhibition of bacteria by QDs.[48,49]

Low biocompatibility is one of the key factors limiting the clinical application of various new materials and technologies.[50] Therefore, this study evaluated the biocompatibility of ZnO@APTES QDs through MTT assay, hemolysis test, and macrophage infection model test. The results showed that ZnO@APTES QDs have no significant effect on macrophages, no obvious damage to red blood cells and exhibit good biocompatibility.

In the past decades, the increase in the prevalence of MRSA has been noticed and the interventions for MRSA infected wounds are becoming more challenging.[51] The results of this study show that ZnO@APTES QDs promote wound healing while killing bacteria. Shu et al synthesized chitosan ZnO QDs (CS-ZnO QDs) for the treatment of MRSA-infected wounds. CS-ZnO QDs facilitated MRSA-infected wound healing by inhibition of bacterial growth. It is consistent with the results of this study.[52]

This study has some limitations, such as insufficient in-depth investigation of the mechanisms and limited evaluation using animal models. Therefore, further research is needed in the future to explore the underlying mechanisms more thoroughly, such as the regulation of MRSA metabolism by ZnO@APTES QDs, its effect on MRSA resistance genes, and its impact on biofilm gene expression. Additionally, more animal models are required to further evaluate its therapeutic efficacy.

Conclusion

In this study, we synthesized a water-soluble ZnO@APTES QDs using a microwave-assisted method. Characterization results showed that the ZnO@APTES QDs had a particle size of 5 nm, and surface modification improved its water solubility. The ZnO@APTES QDs exhibited excellent antibacterial effects against both sensitive and multidrug resistant bacteria and had a strong impact on biofilm formation and mature biofilm removal. Notably, the ZnO@APTES QDs did not induce bacterial tolerance and resistance even after 30 days of repeated treatment, whereas antibiotics caused an increase in bacterial MIC after just 3 days and a 60-fold increase after 30 days. Therefore, the ZnO@APTES QDs have great potential for the treatment of MRSA related infections. The study on antibacterial mechanisms revealed that the positively charged quantum dots interacted with the bacterial surface, affecting membrane fluidity. The ZnO@APTES QDs entered the cells, produced ROS, damaged bacterial DNA, and led to bacterial death. Evaluation in a mouse wound treatment model showed that the ZnO@APTES QDs had efficient antibacterial effects and promoted wound healing, providing a more effective treatment compared to antibiotics. In summary, this study synthesized a highly effective water-soluble ZnO@APTES QDs against MRSA, which exhibits strong antibacterial and therapeutic effects against MRSA and other bacteria, showing great potential and value for development.

Acknowledgment

The authors appreciate the financial support from the State Key Program of National Natural Science of China (U1808202), the NSFC International (regional) Cooperation and Exchange Program (31961143024), Major science and technology projects of Inner Mongolia of China (2019ZD006), Department of Science & Technology of Liaoning province (2022JH5/10400090), the National Natural Science Foundation of China (82074407), Major Public Relations Project of Scientific and Technological Innovation Project of Chinese Academy of Chinese Medical Science (CI2021A01204). 2024 Local Universities' Scientific Research Platform Project Supported by Central Government—Key Laboratory Project for Higher Universities of Inner Mongolia Autonomous Region. Basic Scientific Research Project for Universities of Inner Mongolia Autonomous Region—Capacity Building Project of Scientific Research and Innovation Platform of Brucellosis Prevention and Treatment Engineering Technology Research Center. The authors also would like to thank Editage (www.editage.cn) for English language editing. Thanks Biorender.com for providing us with the materials for creating the graphical abstract.

Author Contributions

All authors made a significant contribution to the work reported, whether that is in the conception, study design, execution, acquisition of data, analysis and interpretation, or in all these areas, took part in drafting, revising or critically reviewing the article, gave final approval of the version to be published, have agreed on the journal to which the article has been submitted; and agree to be accountable for all aspects of the work.

Disclosure

The authors report no conflicts of interest in this work.

References

1. Parmanik A, Das S, Kar B, Bose A, Dwivedi GR, Pandey MM. Current treatment strategies against multidrug-resistant bacteria: a review. *Curr Microbiol*. 2022;79(12):388. doi:10.1007/s00284-022-03061-7
2. Watkins RR, Bonomo RA. Overview: the ongoing threat of antimicrobial resistance. *Infect Dis Clin North Am*. 2020;34(4):649–658. doi:10.1016/j.idc.2020.04.002
3. Naghavi M, Vollset SE, Ikuta KS. Global burden of bacterial antimicrobial resistance 1990-2021: a systematic analysis with forecasts to 2050. *Lancet*. 2024;404(10459):1199–1226. doi:10.1016/S0140-6736(24)01867-1
4. Lakhundi S, Zhang K. Methicillin-resistant staphylococcus aureus: molecular characterization, evolution, and epidemiology. *Clin Microbiol Rev*. 2018;31(4). doi:10.1128/CMR.00020-18
5. Aires-de-Sousa M. Methicillin-resistant staphylococcus aureus among animals: current overview. *Clin Microbiol Infect*. 2017;23(6):373–380. doi:10.1016/j.cmi.2016.11.002
6. Guo Y, Song G, Sun M, Wang J, Wang Y. Prevalence and therapies of antibiotic-resistance in staphylococcus aureus. *Front Cell Infect Microbiol*. 2020;10:107. doi:10.3389/fcimb.2020.00107
7. Abebe AA, Birhanu AG. Methicillin resistant staphylococcus aureus: molecular mechanisms underlying drug resistance development and novel strategies to combat. *Infect Drug Resist*. 2023;16:7641–7662. doi:10.2147/IDR.S428103
8. Rajendiran K, Zhao Z, Pei DS, Fu A. Antimicrobial activity and mechanism of functionalized quantum dots. *Polymers*. 2019;11(10):1670. doi:10.3390/polym11101670
9. Alavi M, Jabari E, Jabbari E. Functionalized carbon-based nanomaterials and quantum dots with antibacterial activity: a review. *Expert Rev Anti Infect Ther*. 2021;19(1):35–44. doi:10.1080/14787210.2020.1810569
10. Bellanger X, Billard P, Schneider R, Balan L, Merlin C. Stability and toxicity of zno quantum dots: interplay between nanoparticles and bacteria. *J Hazard Mater*. 2015;283:110–116. doi:10.1016/j.jhazmat.2014.09.017
11. Jin T, Sun D, Su JY, Zhang H, Sue HJ. Antimicrobial efficacy of zinc oxide quantum dots against listeria monocytogenes, salmonella enteritidis, and Escherichia *coli* o157:h7. *J Food Sci*. 2009;74(1):M46–M52. doi:10.1111/j.1750-3841.2008.01013.
12. Zhu X, Li H, Cai L, et al. Zno nanoparticles encapsulated cellulose-lignin film for antibacterial and biodegradable food packaging. *iScience*. 2024;27(7):110008. doi:10.1016/j.isci.2024.110008
13. Zhang Y, Mu J. Controllable synthesis of flower- and rod-like zno nanostructures by simply tuning the ratio of sodium hydroxide to zinc acetate. *Nanotechnology*. 2007;18(7):75606. doi:10.1088/0957-4484/18/7/075606
14. Wang H, Qian C, Jiang H, Liu S, Yang D, Cui J. Visible-light-driven zinc oxide quantum dots for the management of bacterial fruit blotch disease and the improvement of melon seedlings growth. *J Agric Food Chem*. 2023;71(6):2773–2783. doi:10.1021/acs.jafc.2c06204
15. Wiegand I, Hilpert K, Hancock RE. Agar and broth dilution methods to determine the minimal inhibitory concentration (mic) of antimicrobial substances. *Nat Protoc*. 2008;3(2):163–175. doi:10.1038/nprot.2007.521
16. Kumar A, Singh S, Kumar A, et al. Chemical composition, bactericidal kinetics, mechanism of action, and anti-inflammatory activity of isodon melissoides (Benth.) H. Hara essential oil. *Nat Prod Res*. 2021;35(4):690–695. doi:10.1080/14786419.2019.1591399
17. Hong J, Hu J, Ke F. Experimental induction of bacterial resistance to the antimicrobial peptide tachyplesin i and investigation of the resistance mechanisms. *Antimicrob Agents Chemother*. 2016;60(10):6067–6075. doi:10.1128/AAC.00640-16
18. Haney EF, Trimble MJ, Hancock R. Microtiter plate assays to assess antibiofilm activity against bacteria. *Nat Protoc*. 2021;16(5):2615–2632. doi:10.1038/s41596-021-00515-3
19. Singh K, Hussain I, Mishra V, Akhtar MS. New insight on 8-anilino-1-naphthalene sulfonic acid interaction with tgfnr for hydrophobic exposure analysis. *Int J Biol Macromol*. 2019;122:636–643. doi:10.1016/j.ijbiomac.2018.10.208
20. Grela E, Kozlowska J, Grabowiecka A. Current methodology of mtt assay in bacteria - a review. *Acta Histochem*. 2018;120(4):303–311. doi:10.1016/j.acthis.2018.03.007
21. Sokol MB, Chirkina MV, Yabbarov NG, et al. Structural optimization of platinum drugs to improve the drug-loading and antitumor efficacy of plga nanoparticles. *Pharmaceutics*. 2022;14(11):2333. doi:10.3390/pharmaceutics14112333
22. Rodriguez TE, Garcia RJ, Munoz BJ. Emergence of quinolone-resistant, topoisomerase-mutant Brucella after treatment with fluoroquinolones in a macrophage experimental infection model. *Enferm Infecc Microbiol Clin*. 2015;33(4):248–252. doi:10.1016/j.eimc.2014.03.010
23. Dai T, Tegos GP, Zhiyentayev T, Mylonakis E, Hamblin MR. Photodynamic therapy for methicillin-resistant staphylococcus aureus infection in a mouse skin abrasion model. *Lasers Surg Med*. 2010;42(1):38–44. doi:10.1002/lsm.20887
24. Bellanger X, Schneider R, Dezanet C, et al. Zn (2+) leakage and photo-induced reactive oxidative species do not explain the full toxicity of zno core quantum dots. *J Hazard Mater*. 2020;396:122616. doi:10.1016/j.jhazmat.2020.122616
25. Ramani M, Ponnusamy S, Muthamizhchelvan C, Marsili E. Amino acid-mediated synthesis of zinc oxide nanostructures and evaluation of their facet-dependent antimicrobial activity. *Colloids Surf B Biointerfaces*. 2014;117:233–239. doi:10.1016/j.colsurfb.2014.02.017
26. Huh AJ, Kwon YJ. "Nanoantibiotics": a new paradigm for treating infectious diseases using nanomaterials in the antibiotics resistant era. *J Control Release*. 2011;156(2):128–145. doi:10.1016/j.jconrel.2011.07.002
27. Ciofu O, Moser C, Jensen PO, Hoiby N. Tolerance and resistance of microbial biofilms. *Nat Rev Microbiol*. 2022;20(10):621–635. doi:10.1038/s41579-022-00682-4
28. Ansari MA, Khan HM, Khan AA, Sultan A, Azam A. Characterization of clinical strains of MSSA, MRSA and MRSE isolated from skin and soft tissue infections and the antibacterial activity of zno nanoparticles. *World J Microbiol Biotechnol*. 2012;28(4):1605–1613. doi:10.1007/s11274-011-0966-1
29. Lenaz G, Bertoli E, Curatola G, Mazzanti L, Bigi A. Lipid protein interactions in mitochondria. Spin and fluorescence probe studies on the effect of n-alkanols on phospholipid vesicles and mitochondrial membranes. *Arch Biochem Biophys*. 1976;172(1):278–288. doi:10.1016/0003-9861(76)90077-1

30. Lee AS, de Lencastre H, Garau J, et al. Methicillin-resistant staphylococcus aureus. *Nat Rev Dis Primers*. 2018;4:18033. doi:10.1038/nrdp.2018.33
31. Turner NA, Sharma-Kuinkel BK, Maskarinec SA, et al. Methicillin-resistant staphylococcus aureus: an overview of basic and clinical research. *Nat Rev Microbiol*. 2019;17(4):203–218. doi:10.1038/s41579-018-0147-4
32. Chen H, Zhang M, Li B, et al. Versatile antimicrobial peptide-based zno quantum dots for in vivo bacteria diagnosis and treatment with high specificity. *Biomaterials*. 2015;53:532–544. doi:10.1016/j.biomaterials.2015.02.105
33. Zhou Z, Zhang T, Chen Y, et al. Zinc oxide quantum dots may provide a novel potential treatment for antibiotic-resistant streptococcus agalactiae in lama glama. *Molecules*. 2023;28(13). doi:10.3390/molecules28135115
34. You T, You Q, Feng X, Li H, Yi B, Xu H. A novel approach to wound healing: green synthetic nano-zinc oxide embedded with sodium alginate and polyvinyl alcohol hydrogels for dressings. *Int J Pharm*. 2024;654:123968. doi:10.1016/j.ijpharm.2024.123968
35. Architha N, Ragupathi M, Shobana C, et al. Microwave-assisted green synthesis of fl uorescent carbon quantum dots from Mexican mint extract for fe(3+) detection and bio-imaging applications. *Environ Res*. 2021;199:111263. doi:10.1016/j.envres.2021.111263
36. Yao J, Li L, Li P, Yang M. Quantum dots: from fluorescence to chemiluminescence, bioluminescence, electrochemiluminescence, and electrochemistry. *Nanoscale*. 2017;9(36):13364–13383. doi:10.1039/c7nr05233b
37. Zhang W, Lai EPC. Chemical functionalities of 3-aminopropyltriethoxy-silane for surface modification of metal oxide nanoparticles. *Silicon*. 2022;14(12):6535–6545. doi:10.1007/s12633-021-01477-7
38. Rao W, Yue Q, Gao S, et al. Visible-light-driven water-soluble zinc oxide quantum dots for efficient control of citrus canker. *Pest Manag Sci*. 2024;80(6):3022–3034. doi:10.1002/ps.8010
39. Abdelraheem WM, Khairy R, Zaki AI, Zaki SH. Effect of zno nanoparticles on methicillin, vancomycin, linezolid resistance andbiofilm formation in staphylococcus aureus isolates. *Ann Clin Microbiol Antimicrob*. 2021;20(1):54. doi:10.1186/s12941-021-00459-2
40. Wu X, Wang H, Xiong J, et al. Staphylococcus aureus biofilm: formulation, regulatory, and emerging natural products-derived therapeutics. *Biofilm*. 2024;7:100175. doi:10.1016/j.bioflm.2023.100175
41. Lister JL, Horswill AR. Staphylococcus aureus biofilms: recent developments in biofilm dispersal. *Front Cell Infect Microbiol*. 2014;4:178. doi:10.3389/fcimb.2014.00178
42. Li P, Yu M, Ke X, Gong X, Li Z, Xing X. Cytocompatible amphipathic carbon quantum dots as potent membrane-active antibacterial agents with low drug resistance and effective inhibition of biofilm formation. *ACS Appl Bio Mater*. 2022;5(7):3290–3299. doi:10.1021/acsabm.2c00292
43. Devlin H, Fulaz S, Hiebner DW, JP O, Casey E. Enzyme-functionalized mesoporous silica nanoparticles to target staphylococcus aureus and disperse biofilms. *Int J Nanomed*. 2021;16:1929–1942. doi:10.2147/IJN.S293190
44. Pan X, Wang Y, Chen Z, et al. Investigation of antibacterial activity and related mechanism of a series of nano-mg(oh) (2). *ACS Appl Mater Interfaces*. 2013;5(3):1137–1142. doi:10.1021/am302910q
45. Zakharova OV, Belova VV, Baranchikov PA, et al. The conditions matter: the toxicity of titanium trisulfide nanoribbons to bacteria e. Coli changes dramatically depending on the chemical environment and the storage time. *Int J Mol Sci*. 2023;24(9). doi:10.3390/ijms24098299
46. Ahmed B, Solanki B, Zaidi A, Khan MS, Musarrat J. Bacterial toxicity of biomimetic green zinc oxide nanoantibiotic: insights into znonp uptake and nanocolloid-bacteria interface. *Toxicol Res*. 2019;8(2):246–261. doi:10.1039/c8tx00267c
47. Grebowski J, Krokosz A, Puchala M. Membrane fluidity and activity of membrane atpases in human erythrocytes under the influence of polyhydroxylated fullerene. *Biochim Biophys Acta*. 2013;1828(2):241–248. doi:10.1016/j.bbamem.2012.09.008
48. Li Y, Xie S, Xu D, Shu G, Wang X. Antibacterial activity of zno quantum dots and its protective effects of chicks infected withsalmonella pullorum. *Nanotechnology*. 2021;32(50):505104. doi:10.1088/1361-6528/ac2846
49. Saha A, Chakraborti S. Effect of zno quantum dots on escherichia coli global transcription regulator: a molecular investigation. *Int J Biol Macromol*. 2018;117:1280–1288. doi:10.1016/j.ijbiomac.2018.06.001
50. Almeida MB, Galdiano C, Silva BF, Carrilho E, Brazaca LC. Strategies employed to design biocompatible metal nanoparticles for medical science and biotechnology applications. *ACS Appl Mater Interfaces*. 2024;16:67054–67072. doi:10.1021/acsami.4c00838
51. Mergenhagen KA, Starr KE, Wattengel BA, Lesse AJ, Sumon Z, Sellick JA. Determining the utility of methicillin-resistant staphylococcus aureus nares screening in antimicrobial stewardship. *Clin Infect Dis*. 2020;71(5):1142–1148. doi:10.1093/cid/ciz974
52. Shu G, Xu D, Xie S, et al. The antioxidant, antibacterial, and infected wound healing effects of zno quantum dots-chitosan biocomposite. *Appl Surf Sci*. 2023;611:155727. doi:10.1016/j.apsusc.2022.155727